

The Rho GEFs LARG and GEF-H1 regulate the mechanical response to force on integrins

Christophe Guilluy^{1,5}, Vinay Swaminathan^{2,5}, Rafael Garcia-Mata¹, E. Timothy O'Brien³, Richard Superfine³ and Keith Burridge^{1,4}

How individual cells respond to mechanical forces is of considerable interest to biologists as force affects many aspects of cell behaviour¹. The application of force on integrins triggers cytoskeletal rearrangements and growth of the associated adhesion complex, resulting in increased cellular stiffness^{2,3}, also known as reinforcement⁴. Although RhoA has been shown to play a role during reinforcement³, the molecular mechanisms that regulate its activity are unknown. By combining biochemical and biophysical approaches, we identified two guanine nucleotide exchange factors (GEFs), LARG and GEF-H1, as key molecules that regulate the cellular adaptation to force. We show that stimulation of integrins with tensional force triggers activation of these two GEFs and their recruitment to adhesion complexes. Surprisingly, activation of LARG and GEF-H1 involves distinct signalling pathways. Our results reveal that LARG is activated by the Src family tyrosine kinase Fyn, whereas GEF-H1 catalytic activity is enhanced by ERK downstream of a signalling cascade that includes FAK and Ras.

To analyse the effect of force on RhoA activity we used a permanent magnet to apply a constant force on fibronectin-coated beads for different amounts of time. Consistent with what has been found previously^{5,6}, we observed that tensional forces increased RhoA activity (Fig. 1a,b). Pre-incubation with a function-blocking anti- β 1 antibody (P4C10) prevented RhoA activation in response to force (Fig. 1a), indicating that β 1 integrins are the main extracellular matrix (ECM) receptors involved. When cells were incubated with beads coated with arginine–glycine–aspartic acid (RGD) peptides and then subjected to tensile force, similar activation of RhoA was observed (Supplementary Fig. S1a). Likewise, RhoA was activated by pulling on beads coated with an activating anti- β 1 antibody (TS2/16; Supplementary Fig. S1b), whereas no change in RhoA activity was detected when beads were coated with a non-activating anti- β 1 (Supplementary Fig. S1c),

indicating that integrin engagement is necessary for RhoA activation in response to force.

GEFs increase the activity of RhoA by promoting the exchange of GDP for GTP (ref. 7). Considering that the application of force on integrin-based adhesions activates RhoA, we formed a hypothesis that GEFs specific for RhoA may be recruited to the adhesion complex. To test this hypothesis, we isolated adhesion complexes by separating the fibronectin-coated beads from the lysates of cells stimulated with constant force for different amounts of time. As expected, we found vinculin and focal adhesion kinase (FAK), but not tubulin, in the fraction (Supplementary Fig. S1d). Similar to previous studies^{8,9}, we found that force induced recruitment of vinculin to the adhesion complex (Supplementary Fig. S1d). We found that p115, GEF-H1 and LARG (leukaemia-associated Rho GEF) were present in the adhesion complex (Fig. 1c). Interestingly, the application of force induced the recruitment of LARG and GEF-H1 to the adhesion complex, whereas p115 localization at the adhesion complex was unaffected by tension. To ensure that the detection of p115, LARG and GEF-H1 in the adhesion complex was not due to nonspecific association with the beads, we carried out the same experiment with beads coated with an anti-transferrin receptor (TfR). As expected, we were able to detect TfR, but not p115, LARG or GEF-H1, in the bead-associated complex (Supplementary Fig. S1e). Adhesion-mediated activation of LARG and p115 and their colocalization with adhesion proteins have already been demonstrated¹⁰. However, the presence of the microtubule-associated GEF, GEF-H1, in integrin-based adhesion complexes was unexpected. We next investigated whether the activity of these GEFs was affected by mechanical force. We carried out affinity pull-down assays with a nucleotide-free RhoA mutant, RhoA^{G17A}, as described earlier¹¹. This revealed that force applied to fibronectin-coated beads increased LARG and GEF-H1 activities, but had no effect on the activities of several other RhoA GEFs such as Ect2 (epithelial cell transforming

¹Department of Cell and Developmental Biology, University of North Carolina at Chapel Hill, Chapel Hill, North Carolina 27599, USA. ²Curriculum in Applied Sciences and Engineering, University of North Carolina at Chapel Hill, Chapel Hill, North Carolina 27599, USA. ³Department of Physics and Astronomy, University of North Carolina at Chapel Hill, Chapel Hill, North Carolina 27599, USA. ⁴Lineberger Comprehensive Cancer Center, and UNC McAllister Heart Institute, University of North Carolina, Chapel Hill, North Carolina 27599, USA. ⁵These authors contributed equally to this work.

⁷Correspondence should be addressed to K.B. (e-mail: keith_burridge@med.unc.edu)

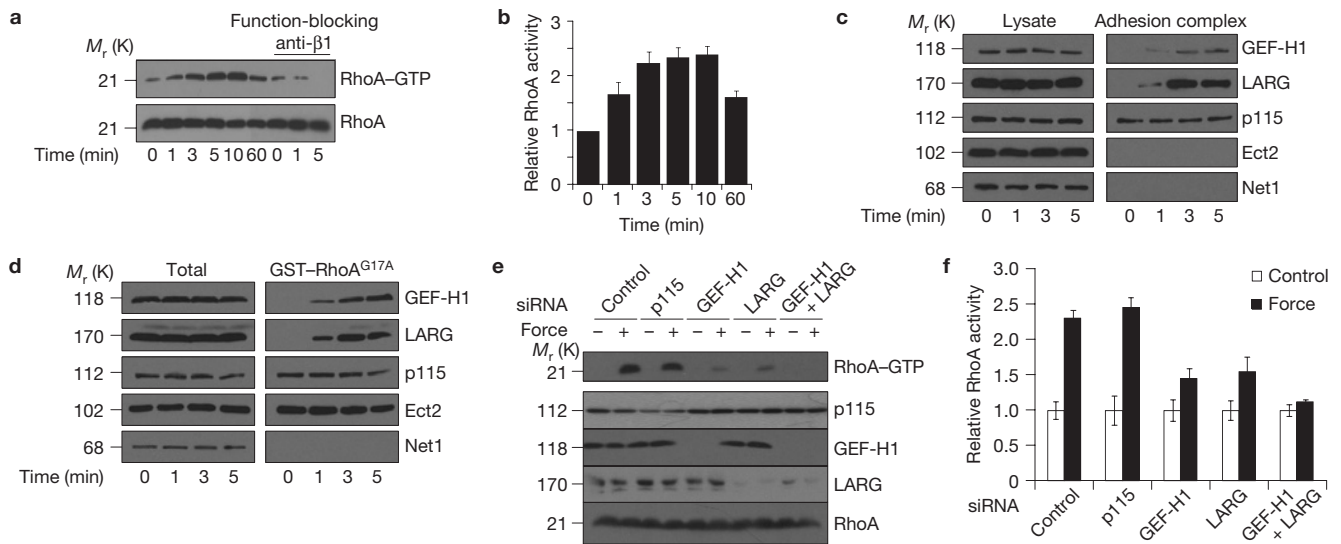


Figure 1 LARG and GEF-H1 activate RhoA in response to force. **(a,b)** REF52 cells were incubated without or with the function-blocking anti- $\beta 1$ antibody (P4C10) for 30 min and then with fibronectin-coated magnetic beads. A permanent magnet was used to generate tensional force for different amounts of time. **(a)** Active RhoA (RhoA-GTP) was isolated with GST-RBD and analysed by western blotting. **(b)** Corresponding densitometric analysis of RhoA-GTP normalized to RhoA levels and expressed relative to the control in the absence of stimulation by force (error bars represent s.e.m., $n = 5$). **(c)** REF52 cells were incubated for 30 min with fibronectin-coated beads and stimulated with tensional force using a permanent magnet for different amounts of time before cell lysis. After magnetic separation of the adhesion complex fraction, the lysate and the adhesion complex fraction were analysed by western blotting. All results are representative of

at least three independent experiments. **(d)** REF52 cells were incubated for 30 min with fibronectin-coated beads and stimulated with tensional force using a permanent magnet for different amounts of time before cell lysis. Active GEFs were sedimented with GST-RhoA^{G17A} and analysed by western blotting. All results are representative of at least three independent experiments. **(e,f)** REF52 cells were transfected for 48 h with control siRNA or siRNA targeting p115, GEF-H1, LARG or both GEF-H1 and LARG, and incubated for 30 min with fibronectin-coated beads. **(e)** After stimulation with tensional force for 5 min, cells were lysed and active RhoA (RhoA-GTP) was isolated with GST-RBD and analysed by western blotting. **(f)** The corresponding densitometric analysis. RhoA-GTP is normalized to RhoA levels and expressed relative to the control (error bars represent s.e.m., $n = 4$). Uncropped images of blots are shown in Supplementary Fig. S5.

sequence 2 oncogene protein), p115 or Net1 (neuroepithelial cell transforming protein 1; Fig. 1d).

To determine whether these GEFs are responsible for RhoA activation in response to force, we depleted their expression using short interfering RNA (siRNA). Depletion of LARG or GEF-H1 significantly decreased RhoA activation in response to force, whereas knockdown of p115 did not affect the force-induced RhoA activation (Fig. 1e,f). Double knockdown of LARG and GEF-H1 totally abrogated RhoA activation. Two independent siRNA duplexes targeting GEF-H1 and LARG generated similar results (data not shown). Integrin-mediated signalling to RhoA is required for rearrangements of the actin cytoskeleton during adhesion. Early adhesion is associated with transient RhoA inhibition and Rac activation, allowing actin protrusion, whereas mature adhesions are associated with the development of RhoA-mediated tension¹². Previous studies have shown that the transient depression in RhoA activity following integrin engagement involves p190RhoGAP (ref. 13), and subsequent activation of RhoA involves p115, LARG and p190RhoGEF (refs 10,14). We show here that the application of force on integrins stimulates the RhoA pathway through an overlapping set of regulators.

We next investigated the role of these GEFs during reinforcement. To study how cells change their mechanical properties in response to mechanical stresses, we used magnetic tweezers to apply controlled force on magnetic beads coated with fibronectin. The local viscoelastic properties of the cells were determined by measuring bead displacements due to a known force induced by a magnetic field¹⁵. Stimulation with successive pulses of constant force triggered a local

change in cellular stiffness, resulting in decreased bead displacement (Fig. 2a). To quantify this local increase in stiffness, the spring constant was calculated for each pulse by fitting the bead displacement and force magnitude to a modified Kelvin-Voigt model^{16,17} (Supplementary Fig. S2). 'Relative cellular stiffness' was calculated by normalizing the spring constant for pulses 2, 3, 4 and 5 to that observed during the first pulse. The change in cellular stiffness was already significant between the first and the second pulse (Supplementary Fig. S3a), demonstrating that cellular adaptation to force on integrins is a rapid phenomenon, as previously reported^{13,4}. Using pharmacological inhibitors, it has been shown that RhoA is involved in reinforcement³. To examine the role of RhoA during cellular stiffening in our system, we depleted RhoA expression using siRNA. On depletion of RhoA expression, the cells showed decreased rigidity (Supplementary Fig. S3b,c). Interestingly, the change in cellular stiffness after the application of pulses of force was no longer detected in the RhoA-knockdown cells (Fig. 2b). Expression of an siRNA-resistant mutant of RhoA in the knockdown cells restored the cellular stiffening in response to force (Fig. 2b). Similar results were obtained when we treated the cells with the RhoA inhibitor C3 transferase (Supplementary Fig. S3d), indicating that RhoA activity is necessary for the cellular adaptation to force. To explore the role of the GEFs during the stiffening response, we depleted their expression using siRNA and monitored the change in cellular stiffness during pulses of force application. We found that knockdown of either p115, LARG, GEF-H1 or Ect2 decreased the basal rigidity of the cells (Supplementary Fig. S3e). Cells depleted of LARG and GEF-H1 suppressed the stiffening response following force application, whereas cells depleted of Ect2 or

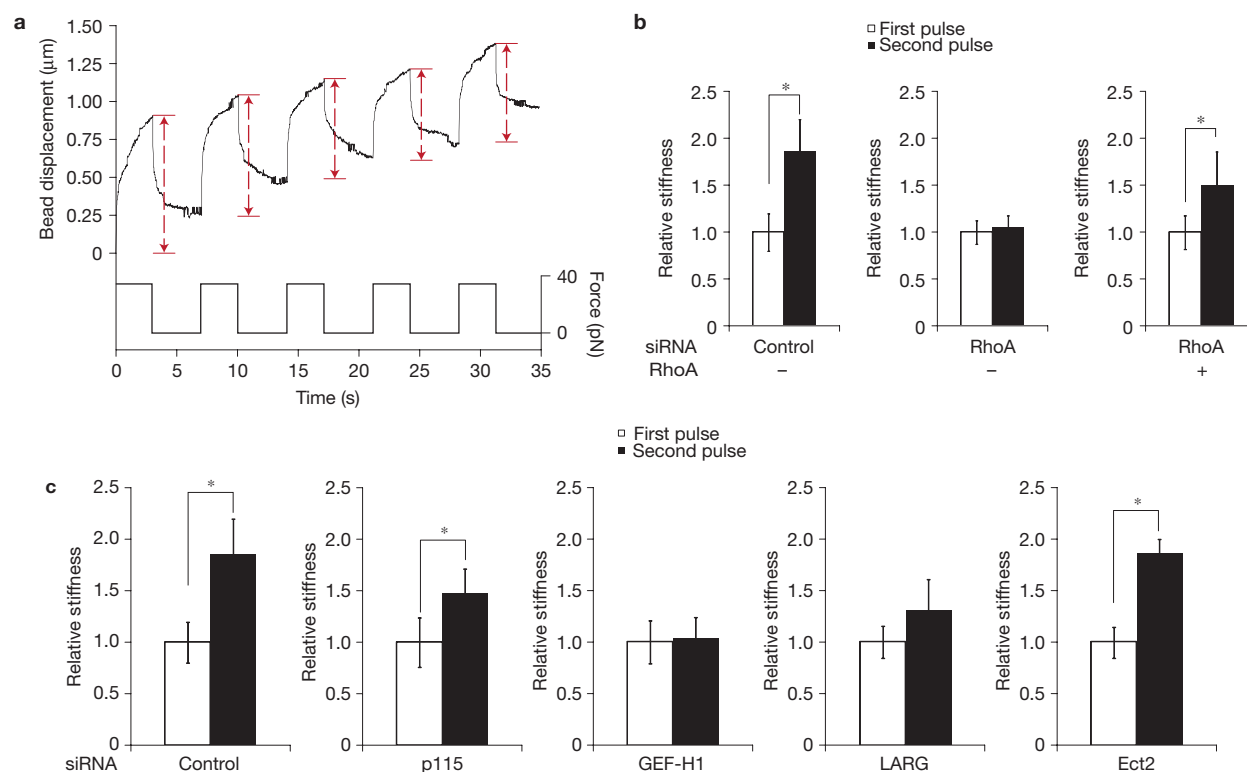


Figure 2 LARG and GEF-H1 mediate cellular stiffening in response to force applied on integrins. **(a)** Typical displacement of a fibronectin-coated bead bound to a REF52 fibroblast during force pulse application. **(b)** Change in stiffness during two force pulses applied to fibronectin-coated beads bound to REF52 cells transfected for 48 h with control siRNA or RhoA siRNA or

RhoA siRNA and an siRNA-resistant mutant of RhoA (myc-RhoA) (error bars represent s.e.m., $n = 20$; $*P < 0.01$). **(c)** Change in stiffness during two force pulses applied to fibronectin-coated beads bound to REF52 cells transfected for 48 h with control siRNA or siRNA targeting p115, GEF-H1, LARG or Ect2 (error bars represent s.e.m., $n = 20$, $*P < 0.05$).

p115 were still able to significantly increase their stiffness in response to force (Fig. 2c). These results indicate that both LARG and GEF-H1 are necessary for cells to adjust their mechanical properties in response to force applied to integrins. We cannot rule out a potential role for p115 in this response, because the knockdown was never as efficient (Fig. 1e and Supplementary Fig. S3f) as for LARG and GEF-H1 and because p115 knockdown did decrease the stiffening response (Fig. 2c).

Src family kinases (SFKs) have been shown to be activated in response to force¹⁸ and to contribute to cellular stiffening in response to force³. To test whether SFKs are involved in LARG and GEF-H1 activation by force, we used the SFK inhibitor SU6656. Pharmacological inhibition of SFKs completely prevented LARG activation in response to force (Fig. 3a), but had no effect on GEF-H1 activation, indicating that GEF-H1 and LARG are activated through two independent mechanisms. Consistent with this, inhibition of SFKs by SU6656 decreased the level of RhoA activation in response to force (Fig. 3b). To identify which SFK member is responsible for LARG activation by force, we used the SYF cells (deficient in Src–Yes–Fyn tyrosine kinases). Applying force on fibronectin-coated beads adhering to SYF^{-/-} cells did not increase LARG activity (Fig. 3c), whereas it stimulated GEF-H1 activity. Surprisingly, expression of Src in the SYF^{-/-} cells did not rescue activation of LARG (Fig. 3c). However, re-expression of Fyn in SYF^{-/-} cells did restore LARG activation in response to force. Consistent with this observation, analysis of the mechanical properties of SYF cells revealed that only SYF^{-/-} cells re-expressing Fyn but not Src showed a significant increase in stiffness following the application of tension on fibronectin-coated

beads (Fig. 3d). We examined whether differences in activity between Fyn and Src in the SYF cells could explain these results, but found that both Src and Fyn are activated by force (Supplementary Fig. S4a). It has been reported that LARG can be activated by FAK phosphorylation on tyrosine¹⁹. Interestingly, we observed that the level of LARG phosphorylation on tyrosine was increased in response to force (Supplementary Fig. S4b) and SFK inhibition prevented this increase. However, we found that FAK inhibition did not affect LARG activation by force (Fig. 4c), indicating that Fyn activates LARG in a FAK-independent manner. Fyn has been shown to co-localize at adhesion complexes and to play a role in ECM rigidity sensing²⁰. Cells on rigid substrates had more stress fibres²¹ and applied more tension on the ECM through their focal adhesions²². This indicates that the Fyn–LARG pathway may be stimulated by both cell-generated tension as well as by externally applied force, in both cases contributing to increased cellular stiffness.

GEF-H1 has been shown to be regulated by microtubule binding²³, coupling microtubule depolymerization with RhoA activation in multiple cellular processes, such as endothelial barrier permeability, migration and dendritic spine morphology²⁴. To test whether GEF-H1 activation could result from microtubule depolymerization, we pretreated cells with taxol and analysed GEF-H1 activity using the nucleotide-free RhoA-pulldown assay after the application of force. We found that taxol did not affect GEF-H1 activation by force (Supplementary Fig. S4d). This result indicates that GEF-H1 is activated independently of microtubule dissociation and is consistent with previous work that showed that treatment with taxol does not affect

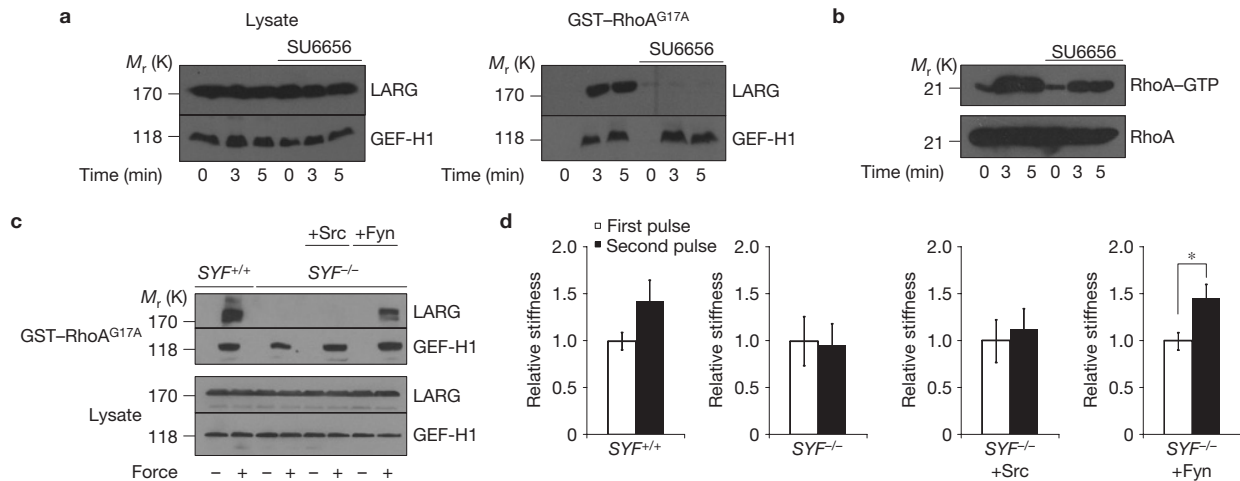


Figure 3 Fyn mediates LARG activation in response to force. **(a)** REF52 cells untreated or treated with SU6656 (2.5 μ M for 30 min) were incubated with fibronectin-coated beads and stimulated with tensional forces for different amounts of time. Active LARG and GEF-H1 were sedimented with GST-RhoA^{G17A} and analysed by western blotting. **(b)** REF52 cells untreated or treated with SU6656 (2.5 μ M for 30 min) were incubated with fibronectin-coated beads. After stimulation with tensional force for different amounts of time, cells were lysed and active RhoA (RhoA-GTP) was isolated with GST-RBD and analysed

by western blotting. **(c)** SYF^{-/-} cells and SYF cells re-expressing Src, Yes and Fyn (SYF^{+/+}) or re-expressing Src or Fyn were incubated with fibronectin-coated beads and stimulated with tensional forces for 3 min. Active LARG and GEF-H1 were pulled down with GST-RhoA^{G17A} and analysed by western blotting. **(d)** Change in stiffness during two force pulses applied to fibronectin-coated beads bound to SYF^{-/-} cells and SYF cells re-expressing Src, Yes and Fyn (SYF^{+/+}) or re-expressing either Src or Fyn (error bars represent s.e.m., **P* = 0.01; *n* = 20). Uncropped images of blots are shown in Supplementary Fig. S5.

RhoA-dependent stress fibre formation in response to stretch⁶. Recent work has shown that the mitogen-activated protein kinase (MAPK) extracellular signal-regulated kinase (ERK) can phosphorylate and activate GEF-H1 (refs 25,26). To test whether ERK is necessary for GEF-H1 activation in response to force, we used the MEK inhibitor U0126. MEK inhibition prevented GEF-H1 activation by tensional force (Fig. 4a), but had no effect on LARG activation, confirming that two distinct pathways turn on these two GEFs. ERK has been shown to phosphorylate GEF-H1 on threonine²⁵. Consistent with this, GEF-H1 was phosphorylated on threonine in response to force and MEK inhibition prevented GEF-H1 phosphorylation (Supplementary Fig. S4e).

We next tested whether force on integrins activates ERK and its canonical upstream regulator Ras. We observed that ERK and Ras are rapidly activated in response to tensional forces (Fig. 4b). It has been shown that integrin-mediated cell adhesion causes activation of the Ras-MAPK pathway, but this activation has been reported to be both dependent on²⁷ and independent of²⁸ FAK. We found that FAK inhibition completely abolished ERK and Ras activation by force (Fig. 4b). When we examined GEF-H1 and LARG activation in response to force we found, as expected, that FAK inhibition prevented GEF-H1 activation and had no effect on LARG activity. This result demonstrates that force on integrins activates GEF-H1 through a signalling cascade that includes FAK, Ras and ERK. It has been shown that complete activation of FAK during integrin-mediated adhesion requires phosphorylation on Tyr 576–577 by Src (ref. 29). Surprisingly, inhibition of SFKs did not affect GEF-H1 activation by force (Fig. 3a). Moreover, SFK inhibition did not prevent Ras and FAK activation in response to force (Supplementary Fig. S4f), indicating that force-mediated FAK activation does not require Src. Analysis of the mechanical properties of cells pretreated with U0126 revealed that MEK inhibition prevented the significant increase in stiffness following the application of tension on fibronectin-coated beads (Fig. 4d).

To measure the role of the GEFs in the stiffening response, we used short pulses of force applied to integrins, whereas to measure their contribution to RhoA activation it was necessary to use longer sustained forces. GEF-H1 and LARG are involved in both the stiffening and the sustained RhoA activation, but there is an interesting difference between these two readouts. With the RhoA measurements, inhibiting one of the GEFs decreased the response but did not abolish it (Fig. 1e,f). Similarly, blocking the respective upstream signalling pathways led to a decrease in the level of RhoA activation, but only to an intermediate level (Fig. 3b and Supplementary Fig. S4g). However, when we examined the stiffening response, inhibiting either pathway blocked the stiffening response (Figs 2c, 3d and 4d). We suspect that the difference reflects that for stiffening to occur in the short time frame following single pulses, the level of RhoA activation beneath a bead has to reach a certain threshold and that this requires both signalling pathways and both GEFs to be activated.

The MAPKs are known to control gene expression, differentiation and growth in response to growth factors³⁰. Here we report that the Ras-MAPK pathway is activated in response to force on integrins and contributes to reinforcement by activating GEF-H1. Recent work has shown that FAK and ERK are activated when cells are grown on rigid substrates^{31,32} and contribute to the malignant phenotype observed in breast cancer cells. Our results demonstrate that GEF-H1 acts downstream of the Ras-MAPK pathway to increase cellular rigidity, indicating that GEF-H1 participates in the control of cellular stiffness in response to substrate rigidity and potentially plays a central role during solid cancer development. Knockdown of GEF-H1 has been reported to not alter the generation of focal adhesions^{14,33} but to modify their growth. Externally applied forces³⁴ as well as cell-generated tension^{9,35} are known to play a critical role during the growth of focal adhesions. This indicates that force experienced by focal adhesions, whether externally applied or generated

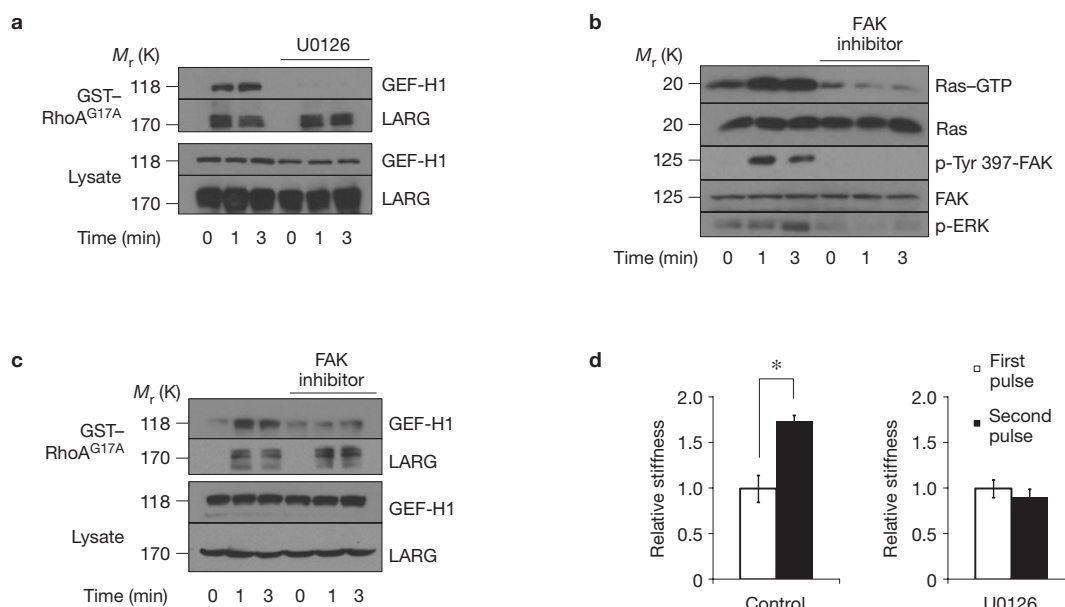


Figure 4 ERK activates GEF-H1 in response to force. **(a)** REF52 cells untreated or treated with U0126 (5 μ M for 30 min) were incubated with fibronectin-coated beads and stimulated with tensional forces for different amounts of time. Active LARG and GEF-H1 were sedimented with GST-RhoA^{G17A} and analysed by western blotting. **(b)** REF52 cells untreated or treated with the FAK inhibitor 14 (5 μ M for 30 min) were incubated with fibronectin-coated beads and stimulated with tensional forces for different amounts of time. Active Ras (Ras-GTP) was sedimented with Raf1-GST. Phosphorylated FAK (Tyr 397), phosphorylated ERK (Thr202 and Tyr204)

and total FAK were analysed by western blotting. **(c)** REF52 cells untreated or treated with the FAK inhibitor 14 (5 μ M for 30 min) were incubated with fibronectin-coated beads and stimulated with tensional forces for different amounts of time. Active LARG and GEF-H1 were sedimented with GST-RhoA^{G17A} and analysed by western blotting. **(d)** Change in stiffness during two force pulses applied to fibronectin-coated beads bound to REF52 cells treated with or without U0126 (5 μ M for 30 min; error bars represent s.e.m., * $P < 0.01$; $n = 20$). Uncropped images of blots are shown in Supplementary Fig. S5.

by the actomyosin contractility, activates GEF-H1, which in turn may regulate the maturation of focal adhesions. This potential role in linking force to focal adhesion maturation could explain why depletion of GEF-H1 and MEK inhibition affect migration as previously reported^{33,36}.

The external mechanical and stress environment of the cell impacts cell differentiation and gene expression³⁷. The mechanical stiffness of the cell will determine its own strain distribution and hence the specific manner and degree of its mechanically activated signalling. Cytoskeletal stiffening in response to force presumably represents an adaptation that allows a cell to modulate its own mechanically active biochemical network within a mechanical feedback loop. Our identification here of two Rho GEFs that become activated downstream from force applied to integrins increases our understanding of these adaptive pathways. It will be interesting in the future to investigate the universality of these pathways and to determine whether the same or different GEFs are also activated when force is transduced by other cell-surface receptors. □

METHODS

Methods and any associated references are available in the online version of the paper at <http://www.nature.com/naturecellbiology>

Note: Supplementary Information is available on the Nature Cell Biology website

ACKNOWLEDGEMENTS

The authors would like to thank L. Sharek for her technical support. This study was supported by National Institutes of Health Grant nos GM029860 and GM029860-28S (to K.B.), P41-EB002025-23A1 (R.S.) and R01-HL077546-03A2 (R.S.), and a grant from the University Cancer Research Fund from the Lineberger Comprehensive Cancer Center. C.G. is supported by a Marie Curie Outgoing

International Fellowship from the European Union Seventh Framework Programme (FP7/2007–2013) under grant agreement no. 254747.

AUTHOR CONTRIBUTIONS

C.G. and V.S. designed and carried out experiments. R.G.M. and E.T.O. helped with experimental design and procedures. C.G. and K.B. wrote the manuscript. K.B. and R.S. directed the project and revised the manuscript. All authors provided detailed comments.

COMPETING FINANCIAL INTERESTS

The authors declare no competing financial interests.

Published online at <http://www.nature.com/naturecellbiology>

Reprints and permissions information is available online at <http://www.nature.com/reprints>

- Hoffman, B. D. & Crocker, J. C. Cell mechanics: dissecting the physical responses of cells to force. *Annu. Rev. Biomed. Eng.* **11**, 259–288 (2009).
- Wang, N., Butler, J. P. & Ingber, D. E. Mechanotransduction across the cell surface and through the cytoskeleton. *Science* **260**, 1124–1127 (1993).
- Matthews, B. D., Overby, D. R., Mannix, R. & Ingber, D. E. Cellular adaptation to mechanical stress: role of integrins, Rho, cytoskeletal tension and mechanosensitive ion channels. *J. Cell Sci.* **119**, 508–518 (2006).
- Choquet, D., Felsenfeld, D. P. & Sheetz, M. P. Extracellular matrix rigidity causes strengthening of integrin-cytoskeleton linkages. *Cell* **88**, 39–48 (1997).
- Zhao, X. H. *et al.* Force activates smooth muscle α -actin promoter activity through the Rho signalling pathway. *J. Cell Sci.* **120**, 1801–1809 (2007).
- Goldyn, A. M., Rioja, B. A., Spatz, J. P., Ballestrem, C. & Kemkemer, R. Force-induced cell polarisation is linked to RhoA-driven microtubule-independent focal-adhesion sliding. *J. Cell Sci.* **122**, 3644–3651 (2009).
- Bos, J.L., Rehmann, H. & Wittinghofer, A. GEFs and GAPs: critical elements in the control of small G proteins. *Cell* **129**, 865–877 (2007).
- Sawada, Y. & Sheetz, M. P. Force transduction by Triton cytoskeletons. *J. Cell Biol.* **156**, 609–615 (2002).
- Pasapera, A. M., Schneider, I. C., Rericha, E., Schlaepfer, D. D. & Waterman, C. M. Myosin II activity regulates vinculin recruitment to focal adhesions through FAK-mediated paxillin phosphorylation. *J. Cell Biol.* **188**, 877–890 (2010).

10. Dubash, A. D. *et al.* A novel role for Lsc/p115 RhoGEF and LARG in regulating RhoA activity downstream of adhesion to fibronectin. *J. Cell Sci.* **120**, 3989–3998 (2007).
11. Garcia-Mata, R. *et al.* Analysis of activated GAPs and GEFs in cell lysates. *Methods Enzymol.* **406**, 425–437 (2006).
12. DeMali, K. A., Wennerberg, K. & Burridge, K. Integrin signalling to the actin cytoskeleton. *Curr. Opin. Cell Biol.* **15**, 572–582 (2003).
13. Arthur, W. T. & Burridge, K. RhoA inactivation by p190RhoGAP regulates cell spreading and migration by promoting membrane protrusion and polarity. *Mol. Biol. Cell.* **12**, 2711–2720 (2001).
14. Lim, Y. *et al.* PyK2 and FAK connections to p190Rho guanine nucleotide exchange factor regulate RhoA activity, focal adhesion formation, and cell motility. *J. Cell Biol.* **180**, 187–203 (2008).
15. Tim O'Brien, E., Cribb, J., Marshburn, D., Taylor, R. M. 2nd & Superfine, R. Chapter 16: magnetic manipulation for force measurements in cell biology. *Methods Cell Biol.* **89**, 433–450 (2008).
16. Bausch, A. R., Moller, W. & Sackmann, E. Measurement of local viscoelasticity and forces in living cells by magnetic tweezers. *Biophys. J.* **76**, 573–579 (1999).
17. Thoumine, O. & Ott, A. Time scale dependent viscoelastic and contractile regimes in fibroblasts probed by microplate manipulation. *J. Cell Sci.* **110**, 2109–2116 (1997).
18. Na, S., Collin, O. & Chowdhury, F. *et al.* Rapid signal transduction in living cells is a unique feature of mechanotransduction. *Proc. Natl Acad. Sci. USA* **105**, 6626–6631 (2008).
19. Chikumi, H., Fukuhara, S. & Gutkind, J. S. Regulation of G protein-linked guanine nucleotide exchange factors for Rho, PDZ-RhoGEF, and LARG by tyrosine phosphorylation: evidence of a role for focal adhesion kinase. *J. Biol. Chem.* **277**, 12463–12473 (2002).
20. Kostic, A. & Sheetz, M. P. Fibronectin rigidity response through Fyn and p130Cas recruitment to the leading edge. *Mol. Biol. Cell.* **17**, 2684–2695 (2006).
21. Pelham, R. J. Jr & Wang, Y. Cell locomotion and focal adhesions are regulated by substrate flexibility. *Proc. Natl Acad. Sci. USA* **94**, 13661–13665 (1997).
22. Mitrossilis, D., Fouchard, J. & Guirouy, A. *et al.* Single-cell response to stiffness exhibits muscle-like behaviour. *Proc. Natl Acad. Sci. USA* **106**, 18243–18248 (2009).
23. Krendel, M., Zenke, F. T. & Bokoch, G. M. Nucleotide exchange factor GEF-H1 mediates cross-talk between microtubules and the actin cytoskeleton. *Nat. Cell Biol.* **4**, 294–301 (2002).
24. Birkenfeld, J., Nalbant, P., Yoon, S. H. & Bokoch, G. M. Cellular functions of GEF-H1, a microtubule-regulated Rho-GEF: is altered GEF-H1 activity a crucial determinant of disease pathogenesis? *Trends Cell Biol.* **18**, 210–219 (2008).
25. Fujishiro, S. H. *et al.* ERK phosphorylate GEF-H1 to enhance its guanine nucleotide exchange activity toward RhoA. *Biochem. Biophys. Res. Commun.* **368**, 162–167 (2008).
26. Kakiashvili, E. *et al.* GEF-H1 mediates tumour necrosis factor- α -induced Rho activation and myosin phosphorylation: role in the regulation of tubular paracellular permeability. *J. Biol. Chem.* **284**, 11454–11466 (2009).
27. Schlaepfer, D. D., Hanks, S. K., Hunter, T. & van der Geer, P. Integrin-mediated signal transduction linked to Ras pathway by GRB2 binding to focal adhesion kinase. *Nature* **372**, 786–791 (1994).
28. Lin, T. H., Aplin, A. E. & Shen, Y. *et al.* Integrin-mediated activation of MAP kinase is independent of FAK: evidence for dual integrin signalling pathways in fibroblasts. *J. Cell Biol.* **136**, 1385–1395 (1997).
29. Frame, M. C., Patel, H., Serrels, B., Lietha, D. & Eck, M. J. The FERM domain: organizing the structure and function of FAK. *Nat. Rev. Mol. Cell Biol.* **11**, 802–814 (2010).
30. Chang, L. & Karin, M. Mammalian MAP kinase signalling cascades. *Nature* **410**, 37–40 (2001).
31. Provenzano, P. P., Inman, D. R., Eliceiri, K. W. & Keely, P. J. Matrix density-induced mechanoregulation of breast cell phenotype, signalling and gene expression through a FAK-ERK linkage. *Oncogene* **28**, 4326–4343 (2009).
32. Paszek, M. J., Zahir, N. & Johnson, K. R. *et al.* Tensional homeostasis and the malignant phenotype. *Cancer Cell.* **8**, 241–254 (2005).
33. Nalbant, P., Chang, Y. C., Birkenfeld, J., Chang, Z. F. & Bokoch, G. M. Guanine nucleotide exchange factor-H1 regulates cell migration via localized activation of RhoA at the leading edge. *Mol. Biol. Cell.* **20**, 4070–4082 (2009).
34. Riveline, D., Zamir, E. & Balaban, N. Q. *et al.* Focal contacts as mechanosensors: externally applied local mechanical force induces growth of focal contacts by an mDia1-dependent and ROCK-independent mechanism. *J. Cell Biol.* **153**, 1175–1186 (2001).
35. Chrzanowska-Wodnicka, M. & Burridge, K. Rho-stimulated contractility drives the formation of stress fibers and focal adhesions. *J. Cell Biol.* **133**, 1403–1415 (1996).
36. Klemke, R. L. *et al.* Regulation of cell motility by mitogen-activated protein kinase. *J. Cell Biol.* **137**, 481–492 (1997).
37. Engler, A. J., Sen, S., Sweeney, H. L. & Discher, D. E. Matrix elasticity directs stem cell lineage specification. *Cell* **126**, 677–689 (2006).

METHODS

Cell lines and reagents. REF52 cells, SYF mouse embryonic fibroblasts and MRC5 cells were grown in Dulbecco's modified Eagle's medium (DMEM; Invitrogen) supplemented with 10% fetal bovine serum (Sigma) and antibiotic-antimycotic solution (Sigma). Taxol, SU6656 and U0126 were purchased from Calbiochem. FAK inhibitor 14 was purchased from Tocris. Cell-permeable C3 transferase was from Cytoskeleton.

Antibodies. The anti-RhoA antibody (26C4, 1:300), anti-Lsc (M-19, 1:500), anti-vinculin (7F9, 1:1,000), anti-transferrin receptor (3B8 2A1, 1:300) and anti-Ect2 (C-20, 1:500) were from Santa Cruz Biotechnology. The antibody against LARG was a kind gift from K. Kaibuchi (Nagoya University, Japan, 1:1,000). Anti-Net1 (1:500) was purchased from Abcam; anti-tubulin (1:2,500) was purchased from Sigma. Anti-phospho Src (Tyr416, 1/1,000), anti-GEF-H1 (1:500) and anti-phospho-threonine-proline (1:500) were purchased from Cell Signaling. Anti-Pan-Ras antibody (OP40, 1:800) was from EMB Chemicals. Anti-Fyn (610163, 1:1,000) was from BD Transduction Laboratories. Function-blocking anti- β 1 integrin (P4C10) was from Millipore.

Purification of recombinant proteins. Construction of the pGEX4T-1 prokaryotic expression constructs containing RhoA^{G17A} (ref. 11) and the Rho-binding domain (RBD) of Rhotekin have been described previously³⁸. The plasmid containing the Raf1-glutathione S-transferase (GST) construct was a kind gift from C.J. Der (University of North Carolina at Chapel Hill). Briefly, expression of the fusion proteins in *Escherichia coli* was induced with 100 μ M isopropyl- β -D-thiogalactoside (IPTG) for 12–16 h at room temperature. Bacterial cells were lysed in buffer containing 50 mM Tris at pH 7.6 (for GST-RBD) or 20 mM HEPES at pH 7.6 (for GST-RhoA^{G17A}), 150 mM NaCl, 5 mM MgCl₂, 1 mM dithiothreitol, 10 μ g ml⁻¹ each of aprotinin and leupeptin, and 1 mM phenylmethyl sulphonyl fluoride, and the proteins were purified by incubation with glutathione-Sepharose 4B beads (GE Healthcare) at 4 °C.

Bead coating and force application. Tosyl-activated magnetic dynabeads (2.8 μ m; Invitrogen) were washed with phosphate buffer and incubated for 24 h with fibronectin or RGD at 37 °C. After three washes with PBS, the beads were sonicated and incubated with cells for 40 min. Coating with antibodies was carried out according to the manufacturer's recommendations (Invitrogen). A ceramic permanent magnet was used to generate perpendicular, tensile forces on beads attached to the dorsal surface of cells. For all experiments, the pole face was parallel with and 0.6 cm from the culture dish surface. At this distance the force on a single bead was 10 pN. A constant force of varying duration was used for all experiments.

Isolation of adhesion complexes. Fibronectin-coated beads were incubated with cells for 40 min and the bound adhesion complexes were isolated in ice-cold lysis buffer (20 mM Tris at pH 7.6, 150 mM NaCl, 0.1% NP-40, 2 mM MgCl₂, 20 μ g ml⁻¹ aprotinin, 1 μ g ml⁻¹ leupeptin and 1 μ g ml⁻¹ pepstatin). Beads were isolated from the lysate using a magnetic separation stand and denatured and reduced in Laemmli buffer.

GST-RBD, GST-Raf1 and GST-RhoA^{G17A} pull-downs. Active RhoA-pull-down experiments were carried out as described elsewhere¹³. REF52 cells were lysed in 50 mM Tris (pH 7.6), 500 mM NaCl, 1% Triton X-100, 0.1% SDS, 0.5% deoxycholate, 10 mM MgCl₂, 200 μ M orthovanadate and protease inhibitors. After removal of the magnetic beads using the magnetic separator (Invitrogen), lysates were clarified by centrifugation at 13,000g, equalized for total volume and protein concentration, and rotated for 30 min with 30 μ g of purified GST-RBD bound to glutathione-Sepharose beads. The bead pellets were washed in 50 mM Tris (pH 7.6), 150 mM NaCl, 1% Triton X-100, 10 mM MgCl₂, 200 μ M orthovanadate, and protease inhibitors, and subsequently processed for SDS-PAGE. For active-Ras-pull-down experiments, cells were lysed in 25 mM Tris (pH 7.6), 150 mM NaCl, 5 mM MgCl₂, 1% NP-40, 5% glycerol and protease inhibitors. Affinity precipitation of exchange factors with the nucleotide-free RhoA^{G17A} mutant has been described in detail previously¹¹. Briefly, cells were lysed in 20 mM HEPES (pH 7.6), 150 mM NaCl, 1% Triton X-100, 5 mM MgCl₂, 200 μ M orthovanadate and protease inhibitors.

Equalized and clarified lysates were incubated with 20 μ g of purified RhoA^{G17A} bound to glutathione-Sepharose beads for 45 min at 4 °C. Samples were then washed in lysis buffer and processed for SDS-PAGE.

Immuno-precipitation. Cells were lysed directly in hot gel sample buffer (200 mM Tris (pH 6.8), 20% glycerol, 4% SDS and 5% 2-ME), and boiled for 10 min. Samples were then diluted with 20 volumes of 1% Triton X-100 and 1% DOC in Tris-buffered saline (TBS). A total of 2 μ g of PY-20 monoclonal anti-phospho-tyrosine antibody and Protein G-Sepharose were added and samples were incubated for 4 h at 4 °C. Samples were then washed five times in 1% Triton X-100 and 1% DOC in TBS, and analysed by western blotting using anti-LARG.

RNA-mediated interference. siRNAs were purchased from the UNC Nucleic Acid Core Facility-Sigma-Genosys (Sigma-Aldrich). The following siRNAs were used in this study: negative control 5'-UCACUCGUGCCGCAUUUCCTT-3'; RhoA-targeted sequence: 5'-GACATGCTTGCTCATAGTCTTC-3'; LARG-Arhgef12 (first duplex)-targeted sequence: 5'-GGACGGAGCTGTAATTGCA-3'; LARG-Arhgef12 (second duplex)-targeted sequence: 5'-TGAAAGAACCCTCGAAACTT-3'; p115-Arhgef1 (first duplex)-targeted sequence: 5'-GGGCTGAGCAGTATCCTAG-3'; p115-Arhgef1 (second duplex)-targeted sequence: 5'-GGCAAGAGGTCATCAGTG-3'; Gef-H1-Arhgef2 (first duplex)-targeted sequence: 5'-CACGTTCCCTTAGTC-3'; Gef-H1-Arhgef2 (second duplex)-targeted sequence: 5'-CACCAAGGCCCT-TAAAGTC-3'; Ect2-targeted sequence: 5'-TGCTGAGAATCTTATGTAC-3'. siRNAs were transfected with Lipofectamine 2000 (Invitrogen).

Magnetic force assay. The UNC three-dimensional force microscope³⁹ (3DFM) was used for applying controlled and precise 60–100 pN local force on the magnetic beads. Cells were plated on coverslips for 24 h and incubated for 40 min after addition of beads. On force application, bead displacements were recorded with a high-speed video camera (Pulnix, JAI) and tracked using Video Spot Tracker (Center for Computer Integrated Systems for Microscopy and manipulation, <http://cismm.cs.unc.edu>). The spring constants were derived by fitting bead displacements and applied force to Jeffrey's model for viscoelastic liquid (Supplementary Fig. S1).

Calculation of spring constant. The UNC 3DFM system was calibrated before experiments using a fluid of known viscosity. Displacement of individual beads attached to cells was tracked using Video Spot Tracker software (Supplementary Fig. S2a,b). Beads that showed displacements of less than 10 nm (detection resolution) and loosely bound beads were not selected for analysis. Custom-made Matlab codes were used to calculate the creep compliance (also referred to as deformability), which is defined as the average time-dependent deformation normalized by the constant stress applied ($J_{\max} = r_{\max} \times 6\pi a/F$, where a is the radius of the bead; Supplementary Fig. S2c). Each compliance curve was then fitted to Jeffrey's model for viscoelastic materials, shown in Supplementary Fig. S2d, using a least-squares method. Stiffness was reported as the value of k in pascals. Subsequent pulses were fitted in the same manner and the average k for each cell type and pulse number was obtained and reported as the mean \pm s.e.m. All statistical analyses including two-tailed Student's t -tests for the P values reported were done in Excel.

Calibration of the permanent magnet system. Calibration of the permanent magnet system was done using previously described methods⁴⁰. Briefly, the magnetic beads were diluted in a fluid of known viscosity and placed in a closed well to eliminate drift. The well was then placed at a known distance from the face of the permanent magnet. Particle velocities were obtained using Video Spot Tracker and in-house Matlab programs from which the applied force was calculated using Stokes's formula.

Statistical analysis. Statistical differences between two groups of data were analysed with a two-tailed unpaired Student t -test.

38. Ren, X. D. *et al.* Regulation of the small GTP-binding protein Rho by cell adhesion and the cytoskeleton. *EMBO J.* **18**, 578–585 (1999).

39. Fisher, J. K., Cribb, J. & Desai, K. V. *et al.* Thin-foil magnetic force system for high-numerical-aperture microscopy. *Rev. Sci. Instrum.* **77**, nihms8302 (2006).

40. Mair, L. *et al.* Size-uniform 200 nm particles: fabrication and application to magnetofection. *J. Biomed. Nanotechnol.* **5**, 182–191 (2009).

DOI: 10.1038/ncb2254

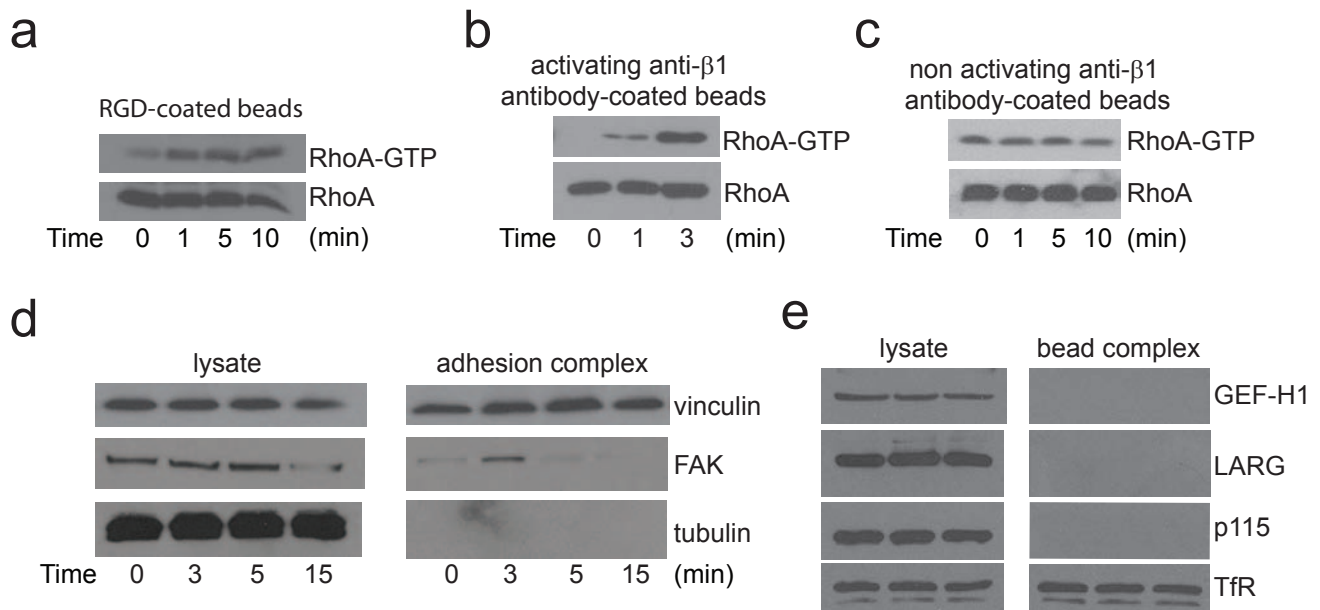


Figure S1 a, REF52 cells were incubated with RGD-coated beads and stimulated with tensional forces for different amounts of time. Active RhoA (RhoA-GTP) was isolated with GST-RBD and analyzed by western blot. b, MRC5 cells were incubated with beads coated with activating anti-β1 integrin antibody (TS2/16) and stimulated with tensional forces for different amounts of time. Active RhoA (RhoA-GTP) was isolated with GST-RBD and analyzed by western blot. c, REF52 cells were incubated with beads coated with non-activating anti-β1 integrin antibody (P4C10) and stimulated with tensional forces for different amounts of time. Active RhoA (RhoA-GTP) was isolated

with GST-RBD and analyzed by western blot. d, REF52 cells were incubated 30 min with FN-coated beads and stimulated with tensional force by using a permanent magnet for different amounts of time. After magnetic separation of the adhesion complex fraction, the lysate and the adhesion complex fraction were analyzed by western blot. e, REF52 cells were incubated with beads coated with anti-TfR antibody and stimulated with tensional forces for different amounts of time. After magnetic separation of the adhesion complex fraction, the lysate and the adhesion complex fraction were analyzed by western blot. All results are representative of at least three independent experiments.

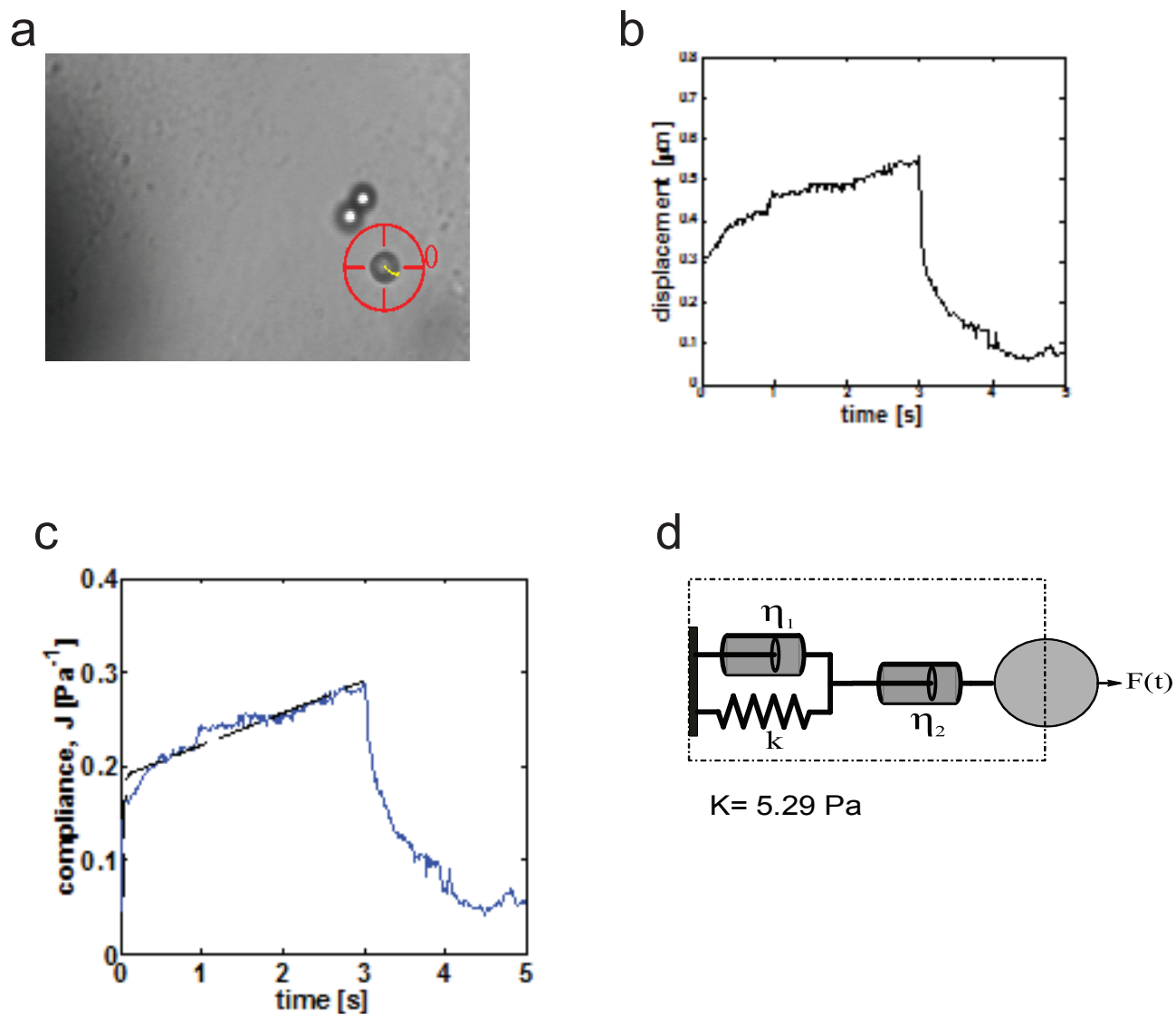


Figure S2 Magnetic tweezer set up and spring constant calculation. a, Experimental setup showing a 2.8 micron fibronectin coated magnetic bead on a cell being pulled by the pole tip. The tracker generated by video spot tracker is used to track bead displacement (magnification 60x). b, Tracked radial displacement shown for the bead pulled by an applied 3 seconds

force. c, The tracked displacement in (b) is converted to compliance as described in the text and then fitted using a least squares method to a Kelvin-Voigt model shown by the dotted line. d, A modified Kelvin-Voigt or Jeffrey's model is shown. All stiffness values reported are the value of the spring constant of the spring k .

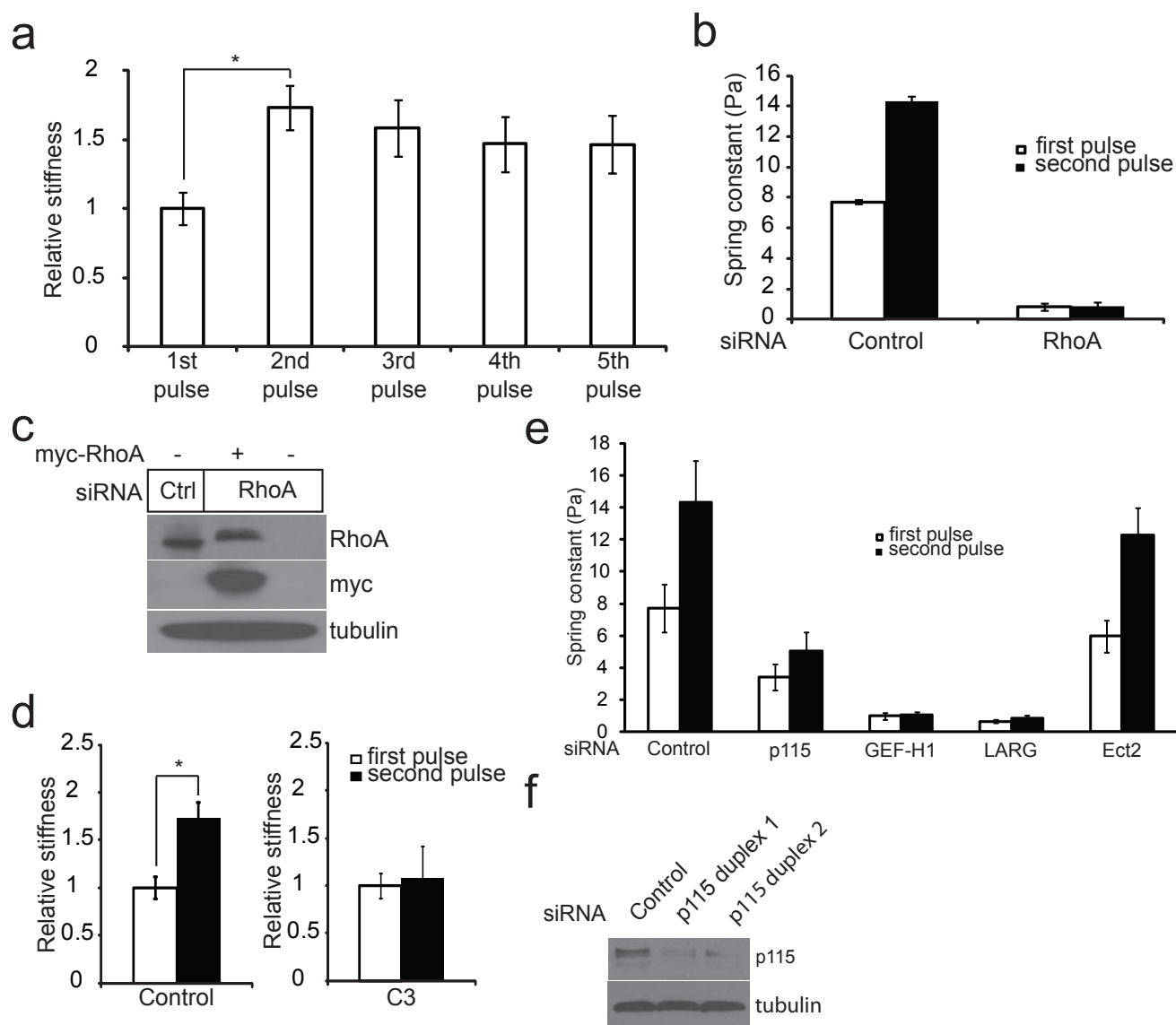


Figure S3 a, Relative change in stiffness of REF52 cells during application of 5 force pulses on FN-coated bead. Spring constant was calculated for each force pulse and expressed as relative to the spring constant observed during the first pulse (error bars represent s.e.m., n=18; * p<0.01). b, Spring constant calculated for the first (white) and second (black) pulse of force applied on FN-coated bead bound to REF52 cells transfected 48 h with control siRNA or RhoA siRNA (error bars represent s.e.m., n=20). c, REF52 cells transfected 48 h with control siRNA or RhoA siRNA or RhoA siRNA and a siRNA-resistant mutant of RhoA (myc-RhoA). Expressions of RhoA, myc and tubulin were analyzed by western blot. d, change in

stiffness during 2 force pulses applied on FN-coated beads bound to untreated REF52 cells (left panel) or REF52 cells treated for 90 min with cell-permeable C3 toxin (2 µg/ml) (right panel) (error bars represent s.e.m., n=15, * p<0.01). e, Spring constant calculated for the first (white) and second (black) pulse of force applied on FN-coated bead bound to REF52 cells transfected 48 h with control siRNA or siRNA targeting p115, Gef-H1, LARG, Ect2 or both LARG and GEF-H1 (error bars represent s.e.m., n=20). f, REF52 cells were transfected 48 h with control siRNA or p115 siRNA (duplex 1) or p115 siRNA (duplex 2). Expressions of p115 and tubulin were analyzed by western blot.

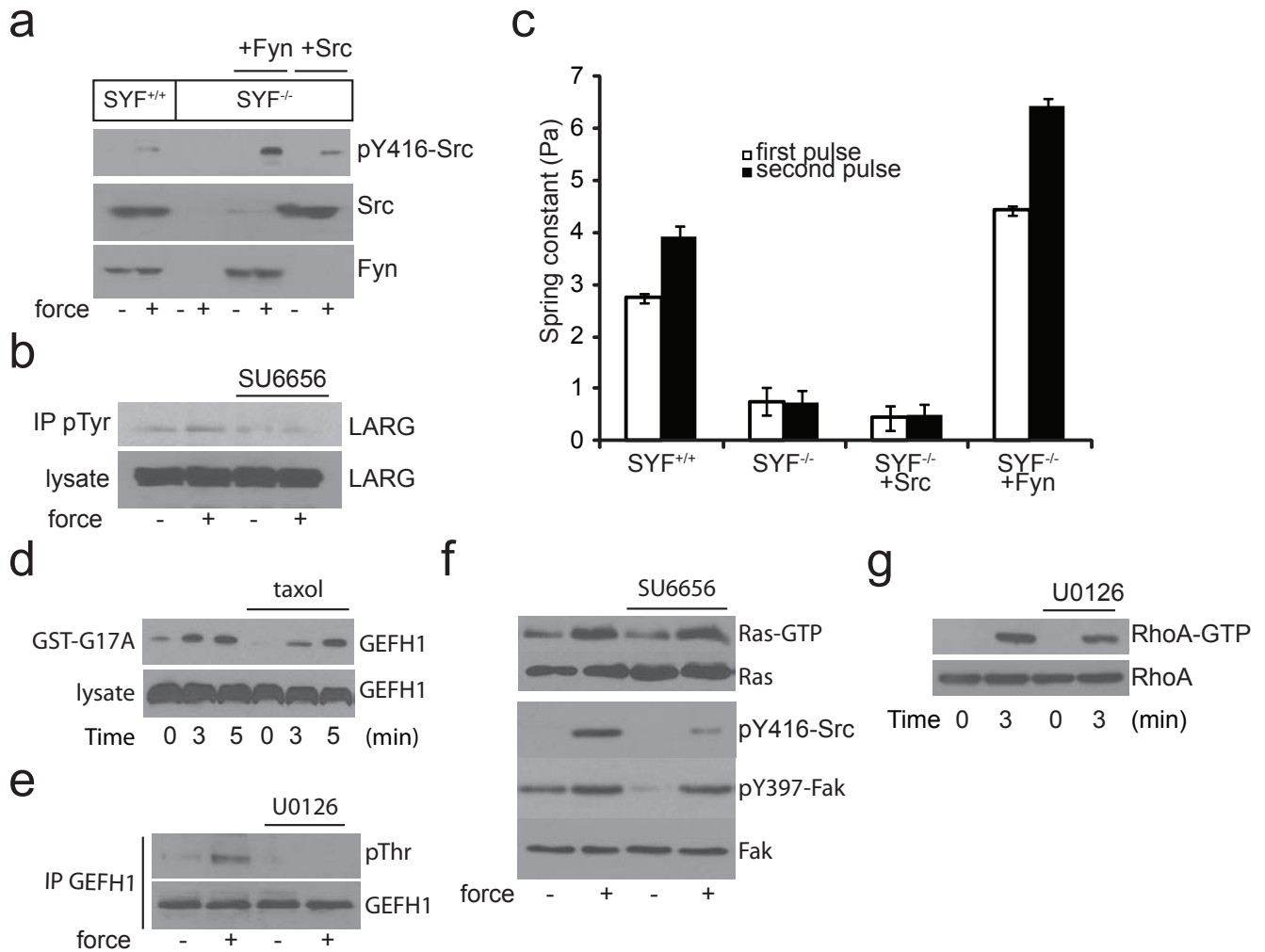


Figure S4 a, SYF^{-/-} cells and SYF cells re-expressing Src, Yes and Fyn (SYF^{+/+}) or re-expressing Src or Fyn were incubated with FN-coated beads and stimulated with force for 3 min. Src and Fyn expressions and activities were analyzed by western blot. b, REF52 cells untreated or treated with SU6656 (2.5 μM for 30 min) were incubated with FN-coated beads and stimulated with force for 3 min. Hot sample buffer was used for lysis. Samples were then diluted to allow immunoprecipitation with anti-phosphotyrosine Ab (PY20). Phosphorylated LARG was analyzed by western blot using anti-LARG antibodies. c, Spring constant calculated for the first (white) and second (black) pulse of force applied on FN-coated bead bound to SYF^{-/-} cells and SYF cells reexpressing Src, Yes and Fyn (SYF^{+/+}) or re-expressing Src or Fyn (error bars represent s.e.m., n=20). d, REF52 cells untreated or treated with taxol (10 μM for 30 min) were incubated with FN-coated beads and stimulated with force for different

amounts of time. Active GEF-H1 was sedimented with GST-RhoAG17A and analyzed by western blot. e, REF52 untreated or treated with U0126 (5 μM for 30 min) were incubated with FN-coated beads and stimulated with forces for 3 min. Immunoprecipitation of GEF-H1 was performed and phosphorylation on threonine was analyzed by western blot using anti-phospho-Threonine-proline antibodies. f, REF52 cells untreated or treated with SU6656 (2.5 μM for 30 min) were incubated with FN-coated beads and stimulated with force for 3 min. Active Ras (Ras-GTP) was sedimented with GST-Raf1. Phosphorylated FAK (Tyr397), phosphorylated Src (Tyr416) and total FAK were analyzed by western blot. g, REF52 cells untreated or treated with U0126 (5 μM for 30 min) were incubated with FN-coated beads. After stimulation with forces for different amounts of time, cells were lysed and active RhoA (RhoA-GTP) was isolated with GST-RBD and analyzed by western blot.

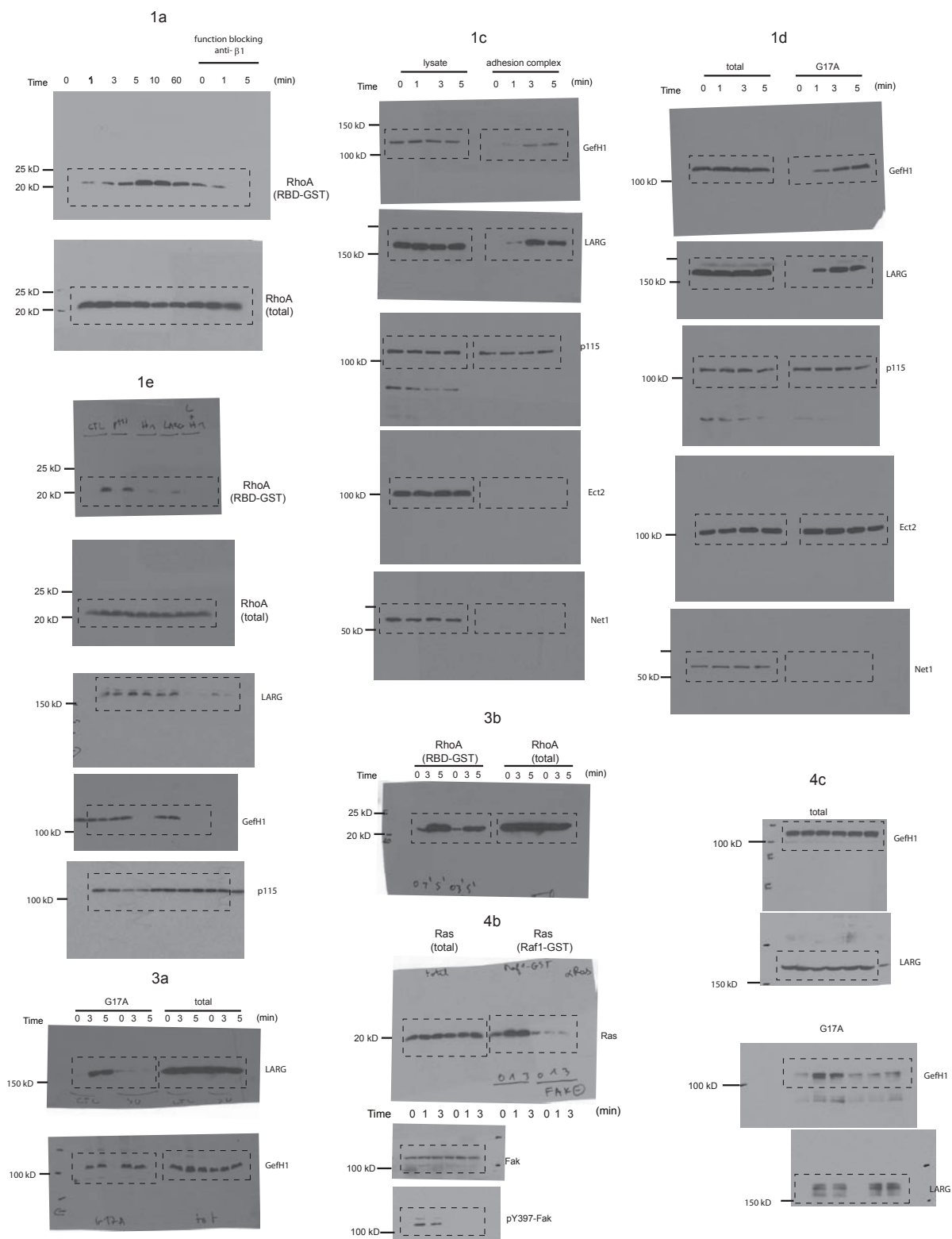


Figure S5 Full scans of gels/blots that have been cropped in Figures within the primary manuscript.

DOI: 10.1038/ncb2254

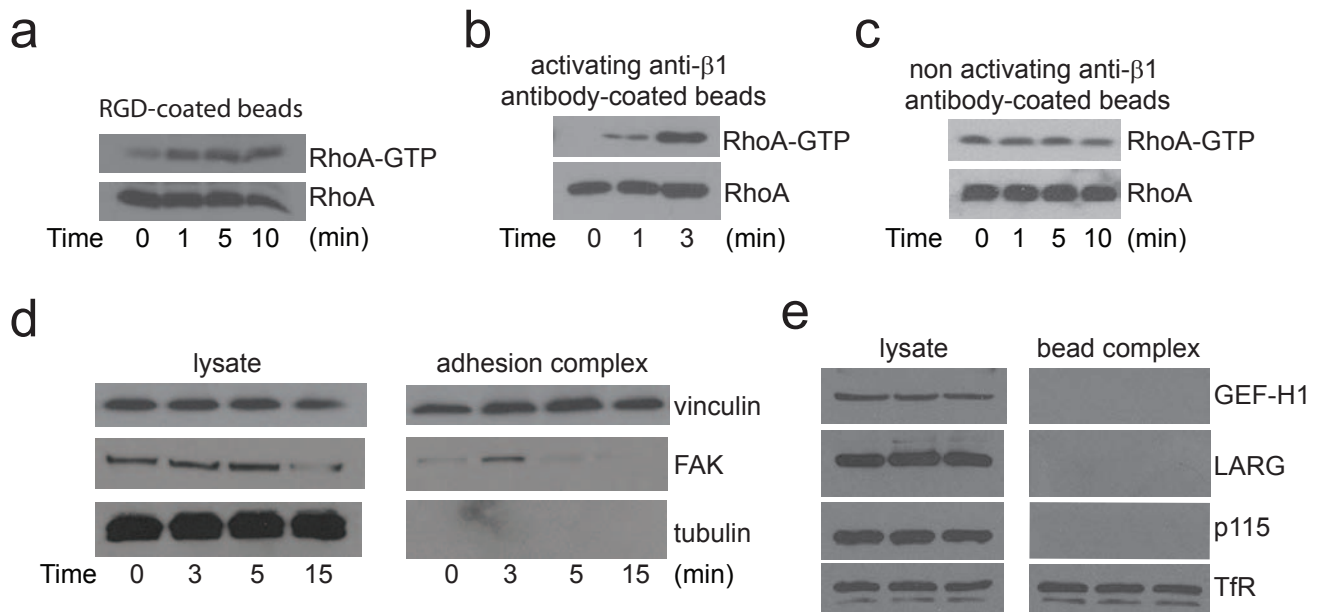


Figure S1 a, REF52 cells were incubated with RGD-coated beads and stimulated with tensional forces for different amounts of time. Active RhoA (RhoA-GTP) was isolated with GST-RBD and analyzed by western blot. b, MRC5 cells were incubated with beads coated with activating anti-β1 integrin antibody (TS2/16) and stimulated with tensional forces for different amounts of time. Active RhoA (RhoA-GTP) was isolated with GST-RBD and analyzed by western blot. c, REF52 cells were incubated with beads coated with non-activating anti-β1 integrin antibody (P4C10) and stimulated with tensional forces for different amounts of time. Active RhoA (RhoA-GTP) was isolated

with GST-RBD and analyzed by western blot. d, REF52 cells were incubated 30 min with FN-coated beads and stimulated with tensional force by using a permanent magnet for different amounts of time. After magnetic separation of the adhesion complex fraction, the lysate and the adhesion complex fraction were analyzed by western blot. e, REF52 cells were incubated with beads coated with anti-TfR antibody and stimulated with tensional forces for different amounts of time. After magnetic separation of the adhesion complex fraction, the lysate and the adhesion complex fraction were analyzed by western blot. All results are representative of at least three independent experiments.

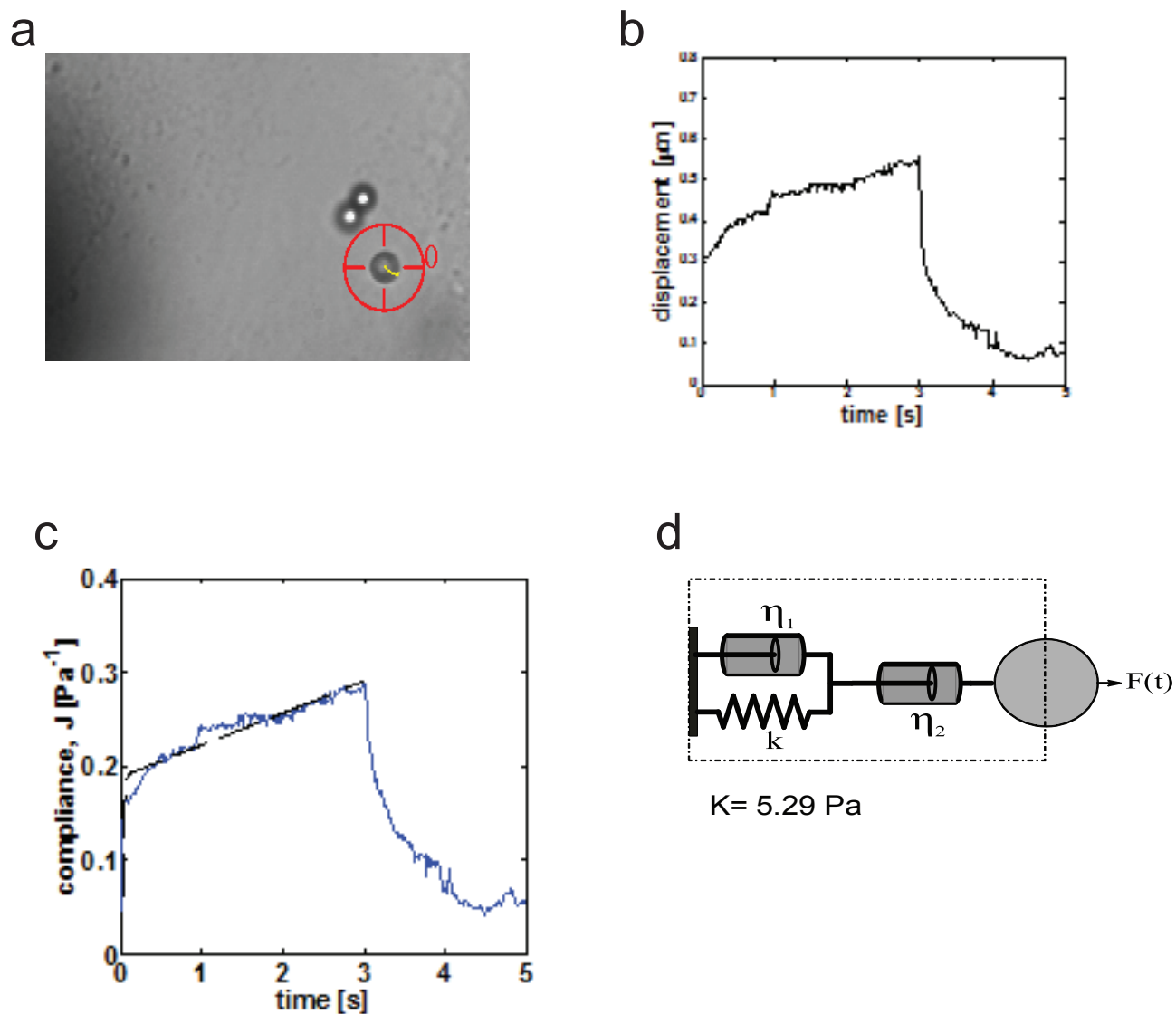


Figure S2 Magnetic tweezer set up and spring constant calculation. a, Experimental setup showing a 2.8 micron fibronectin coated magnetic bead on a cell being pulled by the pole tip. The tracker generated by video spot tracker is used to track bead displacement (magnification 60x). b, Tracked radial displacement shown for the bead pulled by an applied 3 seconds

force. c, The tracked displacement in (b) is converted to compliance as described in the text and then fitted using a least squares method to a Kelvin-Voigt model shown by the dotted line. d, A modified Kelvin-Voigt or Jeffrey's model is shown. All stiffness values reported are the value of the spring constant of the spring k .

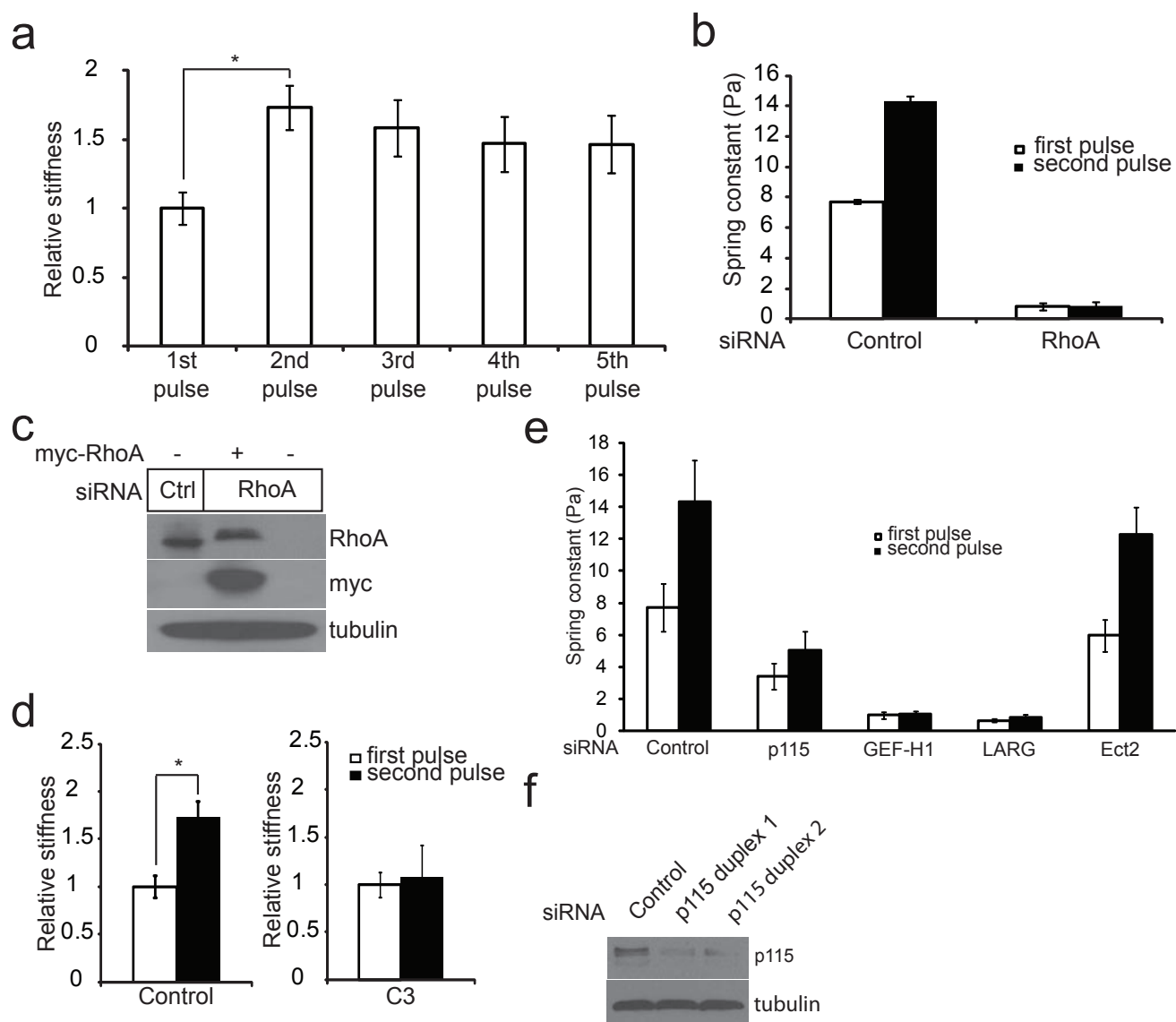


Figure S3 a, Relative change in stiffness of REF52 cells during application of 5 force pulses on FN-coated bead. Spring constant was calculated for each force pulse and expressed as relative to the spring constant observed during the first pulse (error bars represent s.e.m., $n=18$; * $p<0.01$). b, Spring constant calculated for the first (white) and second (black) pulse of force applied on FN-coated bead bound to REF52 cells transfected 48 h with control siRNA or RhoA siRNA (error bars represent s.e.m., $n=20$). c, REF52 cells transfected 48 h with control siRNA or RhoA siRNA or RhoA siRNA and a siRNA-resistant mutant of RhoA (myc-RhoA). Expressions of RhoA, myc and tubulin were analyzed by western blot. d, change in

stiffness during 2 force pulses applied on FN-coated beads bound to untreated REF52 cells (left panel) or REF52 cells treated for 90 min with cell-permeable C3 toxin (2 $\mu\text{g}/\text{ml}$) (right panel) (error bars represent s.e.m., $n=15$, * $p<0.01$). e, Spring constant calculated for the first (white) and second (black) pulse of force applied on FN-coated bead bound to REF52 cells transfected 48 h with control siRNA or siRNA targeting p115, Gef-H1, LARG, Ect2 or both LARG and GEF-H1 (error bars represent s.e.m., $n=20$). f, REF52 cells were transfected 48 h with control siRNA or p115 siRNA (duplex 1) or p115 siRNA (duplex 2). Expressions of p115 and tubulin were analyzed by western blot.

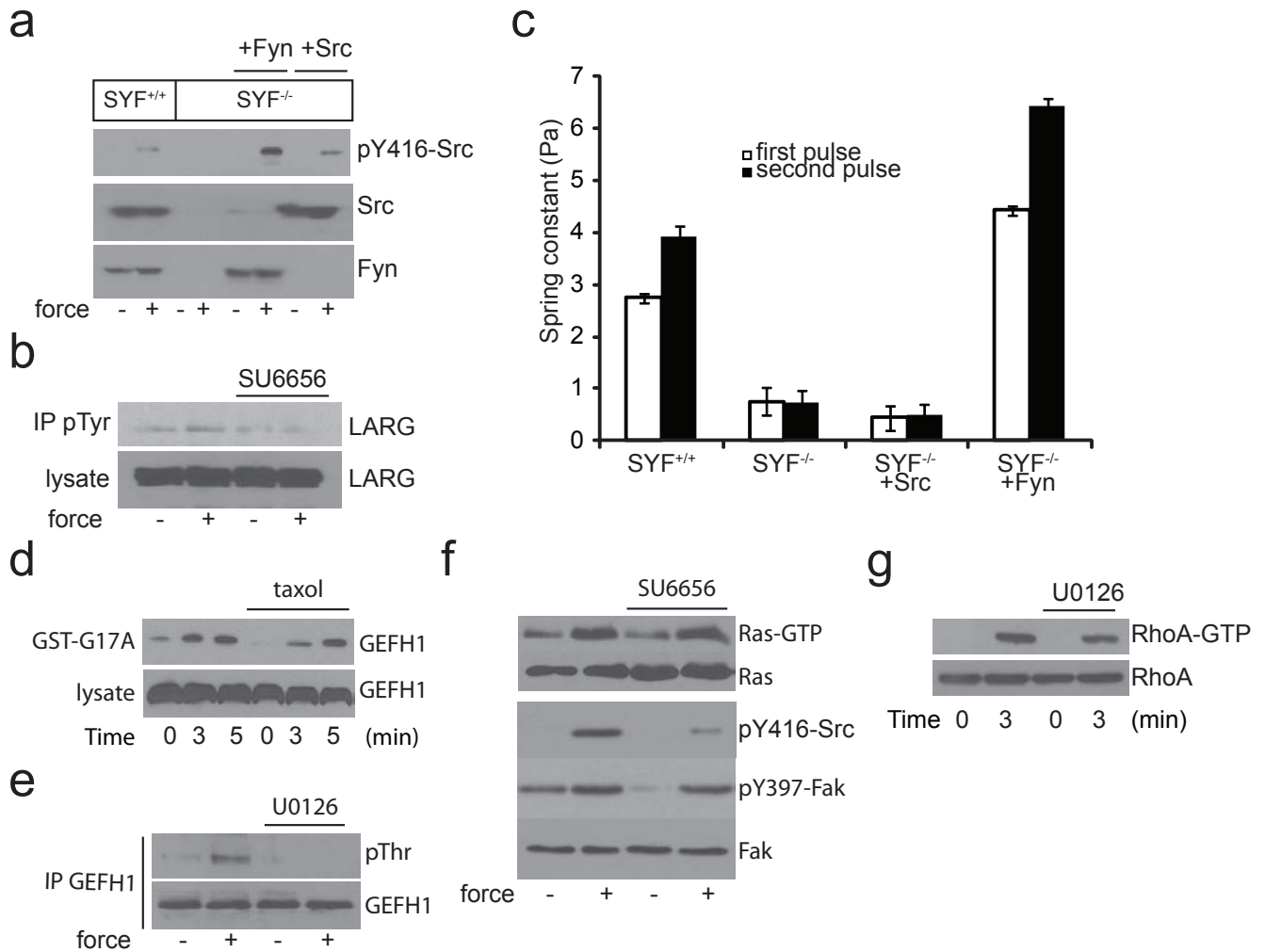


Figure S4 a, SYF^{-/-} cells and SYF cells re-expressing Src, Yes and Fyn (SYF^{+/+}) or re-expressing Src or Fyn were incubated with FN-coated beads and stimulated with force for 3 min. Src and Fyn expressions and activities were analyzed by western blot. b, REF52 cells untreated or treated with SU6656 (2.5 μM for 30 min) were incubated with FN-coated beads and stimulated with force for 3 min. Hot sample buffer was used for lysis. Samples were then diluted to allow immunoprecipitation with anti-phosphotyrosine Ab (PY20). Phosphorylated LARG was analyzed by western blot using anti-LARG antibodies. c, Spring constant calculated for the first (white) and second (black) pulse of force applied on FN-coated bead bound to SYF^{-/-} cells and SYF cells reexpressing Src, Yes and Fyn (SYF^{+/+}) or re-expressing Src or Fyn (error bars represent s.e.m., n=20). d, REF52 cells untreated or treated with taxol (10 μM for 30 min) were incubated with FN-coated beads and stimulated with force for different

amounts of time. Active GEF-H1 was sedimented with GST-RhoAG17A and analyzed by western blot. e, REF52 untreated or treated with U0126 (5 μM for 30 min) were incubated with FN-coated beads and stimulated with forces for 3 min. Immunoprecipitation of GEF-H1 was performed and phosphorylation on threonine was analyzed by western blot using anti-phospho-Threonine-proline antibodies. f, REF52 cells untreated or treated with SU6656 (2.5 μM for 30 min) were incubated with FN-coated beads and stimulated with force for 3 min. Active Ras (Ras-GTP) was sedimented with GST-Raf1. Phosphorylated FAK (Tyr397), phosphorylated Src (Tyr416) and total FAK were analyzed by western blot. g, REF52 cells untreated or treated with U0126 (5 μM for 30 min) were incubated with FN-coated beads. After stimulation with forces for different amounts of time, cells were lysed and active RhoA (RhoA-GTP) was isolated with GST-RBD and analyzed by western blot.

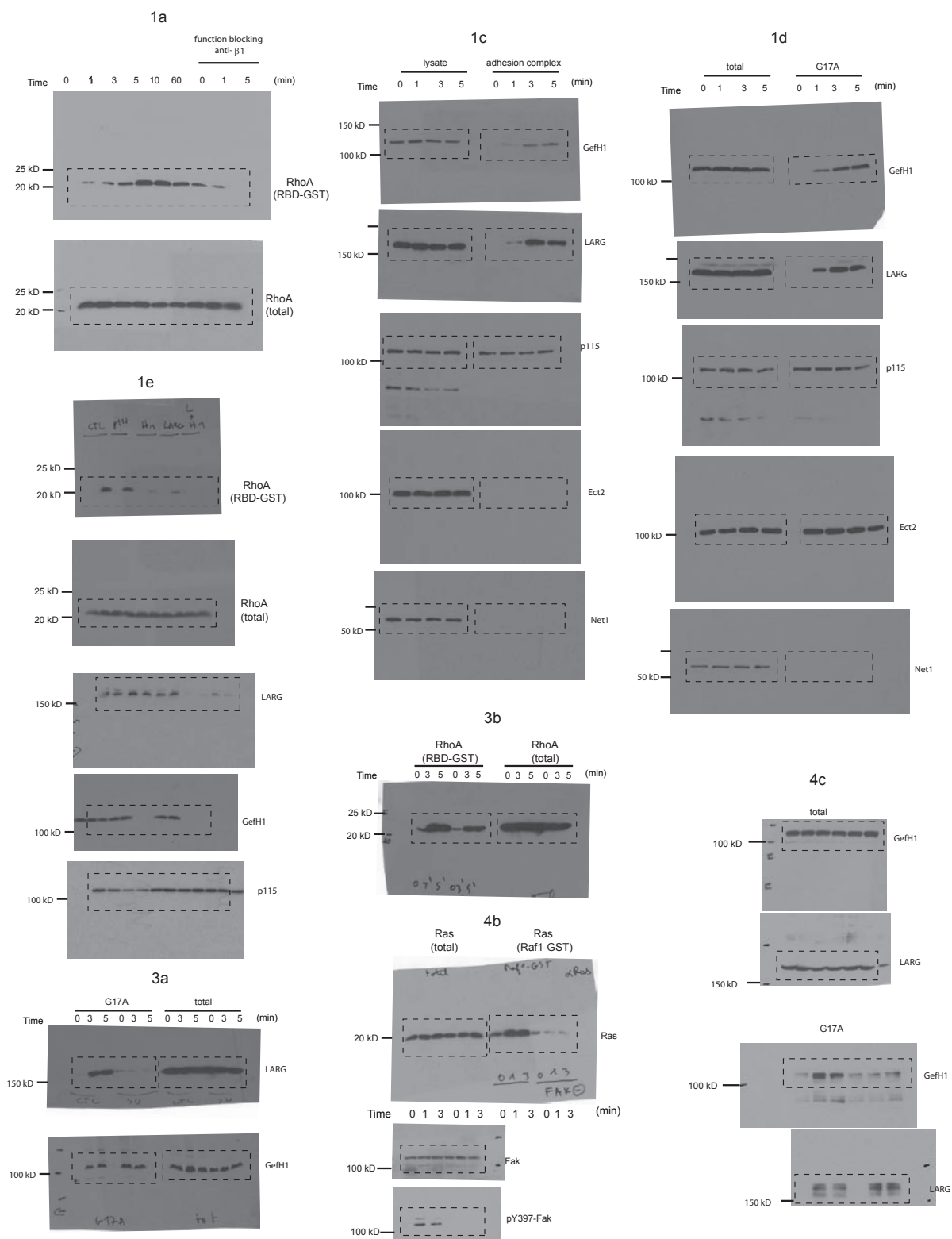


Figure S5 Full scans of gels/blots that have been cropped in Figures within the primary manuscript.